

Modeling Efficiency of InAs-Based Near-Field Thermophotovoltaic Devices

Gavin P. Forcade¹, Christopher E. Valdivia¹, Shengyuan Lu², Sean Molesky³, Alejandro W. Rodriguez³, Jacob J. Krich⁴, Raphael St-Gelais⁵, Karin Hinzer¹

¹ SUNLAB, Centre for Research in Photonics, University of Ottawa, Ottawa, ON, Canada

² Department of Physics, Princeton University, Princeton, NJ, USA

³ Department of Electrical and Computer Engineering, Princeton University, Princeton, NJ, USA

⁴ Department of Physics, University of Ottawa, Ottawa, ON, Canada

⁵ Micro and Nano Systems Lab, University of Ottawa, Ottawa, ON, Canada

Abstract- Enormous potential lies in waste-heat recycling for the world's industrial sector. Portable solid-state modules are a universal low-maintenance method to recycle this waste-heat. One such technology, near-field thermophotovoltaics (NFTPV), relies on a heat source in extreme proximity (<200 nm) to a photovoltaic cell, which then generates electricity. We developed an optoelectronic model where electron-hole pair generation rates are calculated using fluctuation electrodynamics, which we input into an electrical model based in Synopsys TCAD Sentaurus. Using our optoelectronic model, we optimized a novel InAs-based NFTPV device for a 700 K radiator 100 nm away from the PV cell with an efficiency reaching $\sim 17\%$, more than an order of magnitude higher than current NFTPV device efficiencies.

I. INTRODUCTION

In the 2016 Paris Agreement, 191 countries agreed to restrict net greenhouse gas (GHG) emissions to limit the rise in global average temperatures. In addition to transitioning energy production from fossil-fuel sources to renewables, waste-heat recycling technologies provide an enormous potential for GHG reductions via enhanced energy-use efficiency. A quarter of the world's energy consumption originates from the industrial sector, and 55% of its input energy is presently lost as waste heat [1]. Portable solid-state modules that could be directly mounted on any hot surface would provide a universal and straightforward solution to recycle some of this waste heat. For a 900 K heat-source, present waste-heat-to-electricity solid-state converters suffer from low efficiencies of $<12\%$. Novel near-field thermophotovoltaics (NFTPVs) relying on a heat source in extreme proximity, <200 nm, to a photovoltaic (PV) cell, have theoretical efficiencies of 40% for practical devices [2], but cells at room temperature have yet to reach experimental efficiencies $>1\%$ [3], [4].

II. DEVICE

Figure 1 presents our proposed NFTPV module, which converts radiation from a heat source to electrical power. A 700 K microelectromechanical system (MEMS) radiator, consisting of 10^{19} cm⁻³ p-doped silicon, illuminates a favorable narrow-bandgap InAs-based PV cell placed 100 nm away. We optimize for a 700 K MEMS radiator with a 100 nm gap to reflect the achievable working conditions of our MEMS radiator system.

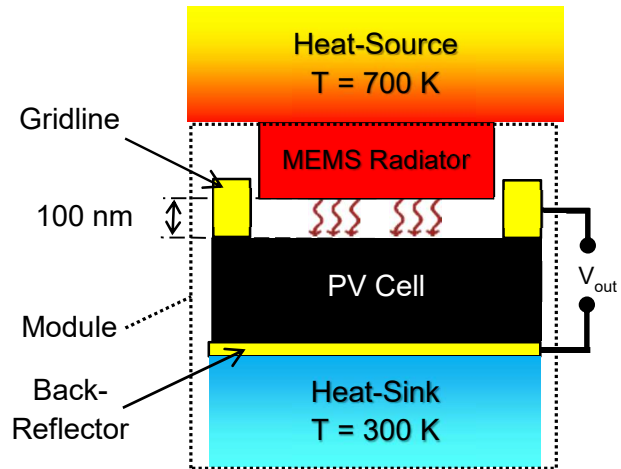


Figure 1 Schematic diagram of our proposed NFTPV module.

In contrast to conventional PV devices, radiation captured by NFTPV cells is both propagative and evanescent, presenting unique design challenges. We explore a novel high-efficiency InAs-based PV cell structure to quench parasitic Auger recombination that dominates in existing cells with p-InAs [5], while also minimizing undesirable diffusion currents. In addition, our structure should reduce surface recombination and top metallization density [6], while a gold back reflector allows for low energy photon recycling.

III. OPTOELECTRONIC MODEL

Depth resolved radiation transport is first determined using in-house fluctuation electrodynamics software [7], [8], where a fluctuating current representing thermal emission is added to Maxwell's equations. The dielectric functions that describe the optical properties of the cell include lattice, free carrier, and interband absorption models. We also include the Moss-Burstein shift, which increases the interband absorption bandgap with increased doping, following the method in [9]. Both the location and optical mechanism by which radiative power transfer occurs are differentiated. Neglecting front contacts, this allows us to calculate a 1D depth-dependent generation profile of electron-hole pairs resulting from interband absorption.

We apply the 1D generation rate profile from our optical simulations throughout the unshaded regions of a 2D cell

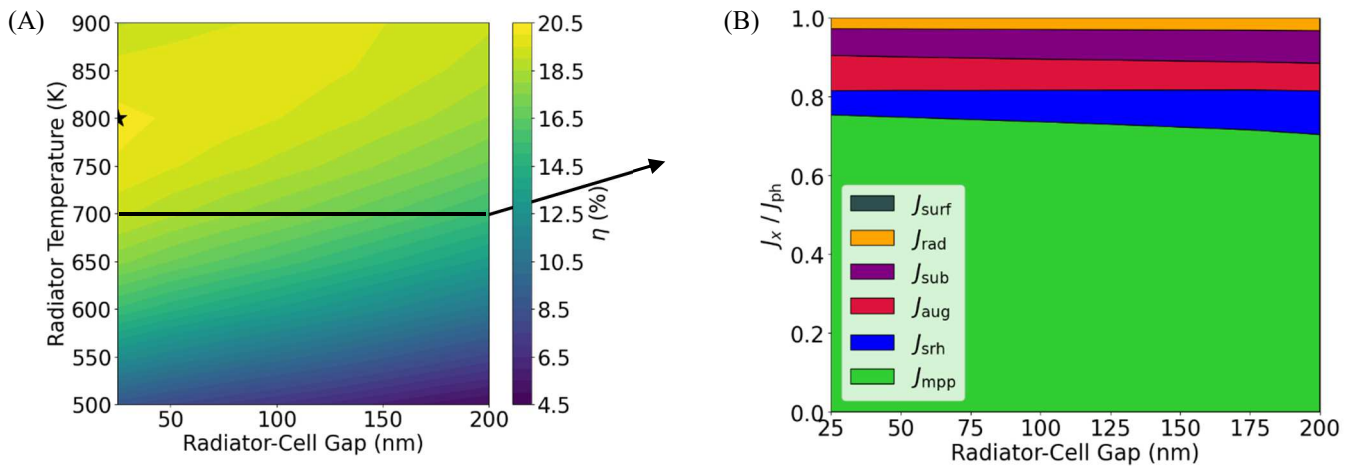


Figure 2 (A) Color plot of system efficiency as a function of radiator-cell separation and radiator temperature. The star represents the maximum calculated efficiency. (B) Currents, at maximum power point, normalized to the total generated current as a function of the radiator-cell separation for 700 K radiator.

structure (Figure 1) in Synopsys TCAD Sentaurus. Our model then solves Poisson’s equation coupled with electron and hole continuity equations to generate depth-resolved recombination rate profiles [10]. We include radiative, Auger, Shockley-Read-Hall (SRH), and surface recombination in our electrical model, and employ the Arora model [11] to compute the doping dependent mobility for majority and minority charge carriers. All ternary and/or quaternary material parameters are interpolated, linearly or using Matthiessen’s rule, between their binary constituents. We also employ bowing parameters for bandgap calculations.

IV. RESULTS

To optimize our device, we maximize the conversion efficiency η , defined as the fraction of total transferred heat converted into electrical power, for a radiator temperature of 700 K and a radiator-cell gap of 100 nm. We optimize the parameter space of layer thicknesses, doping, and stoichiometric ratios of ternary and quaternary materials lattice matched to our InAs substrate. We then explore our device’s performance for a range of radiator temperatures and radiator-cell separations.

Figure 2A displays the system efficiency as a function of radiator-cell separation and radiator temperature for our optimized device. Our system has an efficiency and power output of 17% and $\sim 1 \text{ W/cm}^2$ respectively, for a 700 K radiator with a 100 nm gap. However, the maximum calculated efficiency within the simulation space, 20.5%, is reached for an 800 K radiator 25 nm away from the PV cell with power output $\sim 5 \text{ W/cm}^2$. At lower temperatures and/or larger gaps, the voltage drops due to a lowered generation rate. At higher temperatures and smaller gaps, the cell’s fill factor drops due to non-optimal material bandgap or layer thicknesses for the given operating conditions.

Figure 2B indicates losses by showing current densities J_x associated with a range of processes at maximum power point (MPP) normalized to the total device photogenerated current density J_{ph} for a 700 K radiator. Most photogenerated carriers ($\sim 75\%$) are collected at MPP (J_{mpp}) for all considered gaps. For large radiator-cell gaps, SRH recombination dominates due to a

relatively low generation rate, whereas Auger dominates for small gaps. We also find significant current loss in the substrate (J_{sub}) from light transmitting through the active PV layers, indicating potential efficiency improvements with substrate removal. In this conference, we will present further details on our optoelectronic model, our PV device structure, and results of various parameter optimizations.

REFERENCES

- [1] A. Firth, B. Zhang, and A. Yang, “Quantification of global waste heat and its environmental effects,” *Appl. Energy*, vol. 235, pp. 1314–1334, Feb. 2019, doi: 10.1016/j.apenergy.2018.10.102.
- [2] B. Zhao *et al.*, “High-performance near-field thermophotovoltaics for waste heat recovery,” 2017, doi: 10.1016/j.nanoen.2017.09.054.
- [3] T. Inoue *et al.*, “One-Chip Near-Field Thermophotovoltaic Device Integrating a Thin-Film Thermal Emitter and Photovoltaic Cell,” *Nano Lett.*, vol. 19, no. 6, pp. 3948–3952, Jun. 2019, doi: 10.1021/acs.nanolett.9b01234.
- [4] A. Fiorino *et al.*, “Nanogap near-field thermophotovoltaics,” *Nat. Nanotechnol.*, doi: 10.1038/s41565-018-0172-5.
- [5] Q. Lu *et al.*, “InAs thermophotovoltaic cells with high quantum efficiency for waste heat recovery applications below 1000 °C,” *Sol. Energy Mater. Sol. Cells*, vol. 179, pp. 334–338, Jun. 2018, doi: 10.1016/j.solmat.2017.12.031.
- [6] Y. Sun *et al.*, “Comparing front- and rear-junction GaInP photovoltaic devices through detailed numerical and analytical modeling,” *IEEE J. Photovoltaics*, vol. 9, no. 2, pp. 437–445, Mar. 2019, doi: 10.1109/JPHOTOV.2019.2892530.
- [7] M. T. H. Reid, A. W. Rodriguez, and S. G. Johnson, “Fluctuation-Induced Phenomena in Nanoscale Systems: Harnessing the Power of Noise,” *Proc. IEEE*, vol. 101, no. 2, pp. 531–545, 2013, doi: 10.1109/JPROC.2012.2191749.
- [8] S. Molesky and S. Lu, “heatSlabs,” 2020. <https://github.com/seanMolesky/heatSlabs>.
- [9] D. Milovich *et al.*, “Design of an indium arsenide cell for near-field thermophotovoltaic devices,” *J. Photonics Energy*, vol. 10, no. 02, p. 1, Jun. 2020, doi: 10.1117/1.jpe.10.025503.
- [10] M. M. Wilkins and K. Hinzer, “Multi-junction solar cells, Chapter 40,” in *Handbook of Optoelectronic Device Modeling and Simulation*, vol. 2, 2017.
- [11] N. D. Arora *et al.*, “Electron and Hole Mobilities in Silicon as a Function of Concentration and Temperature,” *IEEE Trans. Electron Devices*, vol. 29, no. 2, pp. 292–295, 1982, doi: 10.1109/T-ED.1982.20698.